Deflection Analysis of an Elastic Single Link Robotic Manipulator

Rafal M. Khalil*   Somer M. Nacy**

*Department of Automated Manufacturing Engineering/ Al-Khwarizmi College of Engineering/ University of Baghdad
**Department of Biomedical Engineering/ Al-Khwarizmi College of Engineering/ University of Baghdad
*E-mail:Rafalalazzawi90@gmail.com
**E-mail :Somernacy@yahoo.com

Abstract

Robotics manipulators with structural flexibility provide an attractive alternative to rigid robotics manipulators for many of the new and evolving applications in robotics. In certain applications their use is unavoidable. The increased complexity in modeling and control of such manipulators is offset by desirable performance enhancements in some respects. In this paperthe single- link flexible robotics manipulator was designed and implemented from Perspex and designed with 0.5 m length , 0.02 m width and with 0.004 m thickness with mass located at the tip. There are four subsystems; motion, control, accelerometer and gyro and a host computer subsystem. The work principle of single-link robotics manipulator is the base servomotor. It rotates a hub with the link on it and measure the tip deflection. the deflection was measured for three cases without load, with 27.5 and with 59.4 gram at the end of the flexible link . During each of the above cases I rotated the base servo motor at an angular velocity equals to 90 deg./s using control card based on ATMEGA640 microcontroller. the deflection was measured for the three cases and the deflection measured by MMA7631 Accelerometer and Gyro . This accelerometer controlled by using MEGA Arduino board . Then the dataI collected collected from accelerometer and plot it using MATLAB software and compared between theoretical results obtained from MATLAB program that based on Lagrange equation of motion and experimental results and we found the maximum deflection occurred when V=180 deg/sec and tip load=59.5 gram.

Keywords: Flexible Link Manipulator , Industrial robotics , Robotics Manipulator ,Beam Deflection.

1. Introduction

Robotic manipulators are used widely to help in dangerous, monotonous, and boring jobs. Most of these robotic manipulators are build and in a manner to maximize stiffness and to minimize the vibration of the end effectors to achieve good position accuracy. The design of high stiffness manipulator is achieved by using heavy material and a bulky design. The existing heavy and rigid manipulators are known to be insufficient in terms of speed and power consumption with respect to the operating payload [1].

To improve industrial productivity of the robotics, it is required to increase the operation speed of the link and/or reduce the weight of the links. Due to high speed operation and lightweight requirements, a dynamic model that includes the joint and / or link flexibilities is needed.

The Link flexibility is a consequence of the lightweight structure in manipulator arms that are modeled and designed to operate at high operation speeds with low inertia. Compared between the conventional heavy and bulky robots and light weight robot, by introducing joints and /or link flexibility on the mechanical system of robots, it has a great advantages of higher operation speed, larger work volume, and lower cost, greater payload-to-manipulator-weight ratio, lower energy consumption, smaller actuators, better transportability, better maneuver ability and at the end of these advantages its safer operation due to reduced inertia [2].

These great disadvantage obtained by introducing joint and / or link flexibilities to robotics mechanical system, that system has high vibration due to low stiffness. If that problem cannot be solved, then the mechanical system of

the robot will not been favored in industries. This will affect the repeatability and accuracy of the end point of manipulator in response to input commands.

To overcome this problem, an accurate dynamic model of the manipulator that can characterize with joint and/or link flexibility has to be developed. This is a first step towards modeling and designing an efficient controlling strategies for these manipulators [3].

Before study of flexible manipulator the construction materials must be focused on , efficient actuation and sensing technologies , and simple and effective controller designs. Flexible robot manipulators are in use in some extent in space applications. This is because of the weight resurrection for a spacecraft ,Other potential areas of application are manipulation in nuclear and other hazardous environment , car/vehicle painting, manufacturing of electronic hardware and food industry[4].

Cannon and Schmitz [5], studied single-link flexible manipulators shown in Fig.1 using the Lagrange's equation and the assumed mode method for modeling the single link manipulator and the vibration is controlled by measuring the position and using strain gauges have been found to be very useful for achieving good performance.
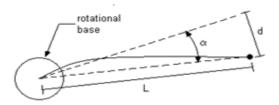

Fig. 1. Flexible Link Manipulator. [1]

Nagarajan and Turcic [6], derived Equations of motion using Lagrange's equation for elastic mechanism systems.

The elastic links are modeled using the finite element method. Both rigid body degrees of freedom and the elastic degrees of freedom are considered as generalized coordinates in the derivation.

Choi et al. [7] ,"addressed the control and the dynamic modeling of a single-link flexible manipulator fabricated from composite laminates (non- metallic) and compared the results with that of aluminum. They have shown that the manipulator fabricated from composite laminates has superior performance characteristics such as

faster settling time, smaller input torque and smaller overshoot relative to the manipulator fabricated from aluminum ". **Choi et al.**[8] , Discussed the utilization of composite materials in the construction of a flexible manipulator to provide higher strength and stiffness-to-weight ratio and larger structural damping than a metallic flexible manipulator .

Krishnamurthy et al. [9], "Present a dynamic model for single-link robotic arms fabricated from orthotropic composite materials. The equations of motion are derived using Hamilton's principle and include the coupling between the rigid body motion and elastic motion. Computer simulated results presented for aluminum, steel, graphite/epoxy, and boron/epoxy indicate that the motion-induced vibration is significantly less for the composite robotic arms as well as substantial savings in energy". So I made our flexible link manipulator from composite material its most preferred because of its light weight and high strength and large structural damping.

2. Characteristics of the Physical Arm

The schematic of a planar single-Link flexible manipulator is shown in Fig. 2, (X_0, Y_0) is an inertial coordinate frame, and (X_1, Y_1) is the coordinate assigned for a flexible link. $\theta, \Psi(x, t)$, an d τ represent the hub position, the deflection do in the arm, and the torque applied to the hub, respectively. The existing experimental single-link flexible manipulator is a 0.5 m long, a flexible structure that can bend in the horizontal plane but it can't bend the vertical plane. At the end of the arm the different load was putted and at the other end was clamped on a rigid hub made from Teflon material mounted directly on the haft of a DC servo motor.

A torque applied by the DC servo motor rotates the arm in a horizontal plane. The other end of the arm with payload mass attached is free. The beam of the manipulator is made of Perspex.
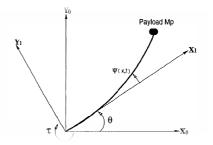

Fig. 2. A Planar Single-Link Flexible Manipulator.

3. Mechanical System Modeling

The equations of motion of this system involving a rotary flexible link manipulator, involves modeling the rigid rotational base and the flexible link together as rigid bodies. a simplification of the partial differential equation describe the motion of a the flexible link, a single degree of freedom approximation in this system is used. At the first start with the derivation of the dynamic model of the system by computing various rotational moments of inertia terms. The rotational inertia for a flexible link is given by:-

$$J_{link} = \frac{1}{3} m_{link} L^2 \qquad \qquad \dots(1)$$

Where: L is the total flexible link length , and m_{link} is the total mass of the flexible link, For a single degree of freedom of this system, the natural frequency is related with torsional stiffness of the link and rotational inertia in the following manner:-

$$\omega_n \sqrt{\frac{K_{stiff}}{J_{link}}} \qquad \qquad \dots(2)$$

Where: ω_{nn} was found experimentally and K_{stiff} is the lateral stiffness constant of the link ,defined as:-

$$K_{stiff} = \frac{F}{\delta} \qquad \qquad \dots(3)$$

Where: F is the force applied at the tip of the link and δ is the tip deflection.

$$\delta = \frac{F L^3}{3 EI} \qquad \qquad \dots(4)$$

And substitutes equation (4) into equation (3) yields the flexural stiffness of cantilever beam :-

$$K_{stiff} = \frac{3 EI}{L^3} \qquad \qquad \dots(5)$$

Where I is the moment of area of the link and E is the young modules of elasticity of the link. In addition, any frictional damping effects between the flexible link and the rotary base was neglected. Next, the generalized dynamic equation of the system was driven for the tip and base using The Lagrange's energy equations of motion in terms of a set of generalized variables phi θ and alpha α ,where α is the angle of tip deflection and θ is the base rotation given in the following:-

$$\frac{\partial}{\partial t}\left(\frac{\partial T}{\partial \theta'}\right) - \frac{\partial T}{\partial \theta} + \frac{\partial P}{\partial \theta} = Q_\theta \qquad \dots(6)$$

Where: P is the total potential energy of the system and T is the total kinetic energy of the system, and Q_i is the ith generalized force within the ith degree of freedom. the virtual forces that applied onto the generalized coordinates obtained from Q_θ and Q_α, be:

$$Q_{\theta = \tau} \qquad \qquad \dots(7)$$
$$Q_\alpha = 0 \qquad \qquad \dots(8)$$

The dynamic equations was driven for the mechanical subsystem from:

$$\ddot{\theta} = -\frac{K_{stiff}}{J_{base}}\alpha + \frac{1}{J_{base}}\tau \qquad \dots(9)$$

$$\ddot{\alpha} = -K_{stiff}\left(\frac{1}{J_{base}} + \frac{1}{J_{base}}\right)\alpha + \frac{1}{J_{base}}\tau \qquad \dots(10)$$

Next, rewriting equations (9) and (10) into a state space form that gives the following equation[10]:

$$\begin{bmatrix} \dot{\theta} \\ \dot{\alpha} \\ \ddot{\theta} \\ \ddot{\alpha} \end{bmatrix} = \begin{bmatrix} 0 & 0 & 1 & 0 \\ 0 & 0 & 0 & 1 \\ 0 & -\frac{K_{stiff}}{J_{base}} & 0 & 0 \\ 0 & -K_{stiff}\left(\frac{1}{J_{base}} + \frac{1}{J_{base}}\right) & 0 & 0 \end{bmatrix} \begin{bmatrix} \theta \\ \alpha \\ \dot{\theta} \\ \dot{\alpha} \end{bmatrix} + \begin{bmatrix} 0 \\ 0 \\ \frac{1}{J_{base}} \\ \frac{1}{J_{base}} \end{bmatrix} \tau$$

$$\dots(11)$$

4. Mathematical Design

Table 1,
Physical parameters of the system.

Parameter	Values
$l* h * b$ (Arm dim.)	0.5 * 0.02 *0.004m
E (Modules of elasticity)	2.1 Gpa
M (link mass)	0.041 kg
Mt (Tip payload)	0, 0.0595,0.0274 kg
Jb(inertia of the base)	0.0229 kg.m^2
T (Motor torque const.)	7,15.5 kg-cm

- T (Torque) = 1.520 N-m
- Kg (motor gear ration) = 2:1
- Vf= (feed voltage)=6 , 12 V

The MATLAB program built to find the tip deflection based on Lagrange equation [10] of motion as mention above and derived using my parameter shown in table 1.1 .the ordinary differential equation (eq.11) solved using Laplace inverse to find the tip deflection.

5. Experimental Work

5.1. Design and Implementation of Single Link Flexible Manipulator

The single link flexible manipulator has been designed and manufactured in the Al-Khwarizmi engineering college workshop; the basic components that have been used to form the flexible manipulator illustrated as following:
(1) High torque servo motor (Changeable Velocities), (2) Teflon Hub with radius (0.0615m), with a width of (0.09 m), (3) Rotating base two layer with radius (0.2m) , with a space between them equal (0.05 m) and thickness equal

(0.005 m). (4) Two aluminum fixed plate, (5) Perspex link with length (0.520 m) , with width of (0.042 m) and with thickness (0.004 m). (6) Power supply to control the velocity of servo motors,(7) MMA 7631 Accelerometer + Gyro sensor to measure the tip deflection of the flexible link, (8) Arduino mega 2560 board to control the accelerometer + gyro, (9) Servo motor control card to control the angle and velocity of the base servo motor . The manufacturing of the flexible link has been done by the following steps: (a) the hub was turning to cylindrical shape with 6.15 mm radius. (b) the Perspex plate was cutting using laser beam cutting to the dimension mention previously . (c) the aluminum plate shaped to fix the Perspex link with the Teflon hub . (d) the Teflon hub with the flexible link mounted above the rotating base and the base servo motor inside the rotating base . (e) Put the load at the end the flexible link and stick the accelerometer on it. The Single link flexible manipulator shown in figures below:

Fig. 3. Hub with rotating base.

The side , front and top view was drawn using AutoCAD software as shown in Figure 4,5,and 6:

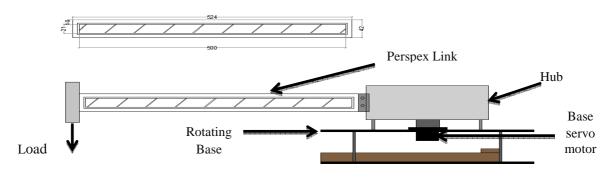**Fig. 4. Flexible link manipulator.**
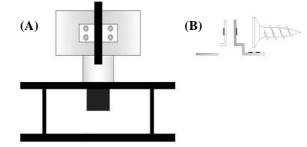

Fig. 5. Flexible link manipulator (Side View).

Fig. 6. (a) Flexible link manipulator (front view), (b) Aluminum fix plate.
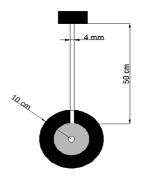

Fig. 7. Flexible link manipulator (top view).

5.2. Control Part

The single link flexible manipulator rotate horizontally using high torque servo motor and this is motor was controlled by servo motor control card based on ATMEGA640. The velocity and the angle of the servo motor controlled through graphical user interface GUI of

servo motion software built in with this card.The MMA7631 Accelerometer + Gyro sensor , its block diagram shown in (Fig. 8).stick at the tip of the link and this is sensor controlled by Arduino Mega 2560 board. The program built using Arduino language and this is language based on C^{++}language .

Fig. 8. Simplified accelerometer functional block diagram.

6. Results and Discussion

6.1. Theoretical Results

The theoretical results obtained from MATLAB software.. The MATLAB program was built based on Lagrange equation. The tip load was changed and the motor velocity also changed and measured the deflection,   as shown in the results below:
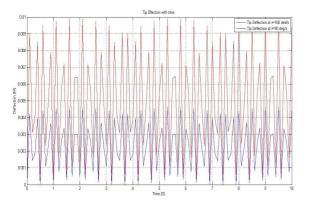
gram. It shows that a time passes, the deflection fluctuates between a values. For v=90 degree/sec. blue curve, Maximum value was found to be (4.6 mm). For v=180 degree/sec. red curve' Maximum value was found to be (9.9 mm).This figure also shows that the maximum tip deflection values decreases as the velocity of the servo motor decrease from 180 to 90 degrees/sec.
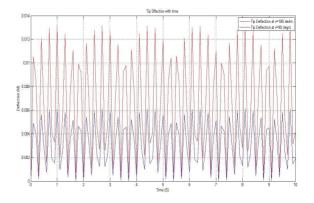

Fig. 10. Tip deflection at tip load=27.4 gram.

Fig. 9. Tip deflection at tip load=0 gram.

Fig. 9 shows the variation of tip deflection with time for two velocity (90 and 180) degree/sec. and for tip attached mass equals zero

Fig. 10 shows the variation of tip deflection with time for two velocity (90 and 180) degree/sec. and for tip attached mass equals 27.4 gram. It shows that a time passes, the deflection fluctuates between a values. For v=90 degree/sec.

blue curve, Maximum value was found to be (6.1 mm). For v=180 degree/sec .red curve, Maximum value was found to be (1.31cm).This figure also shows that the maximum tip deflection values decreases as the velocity of the servo motor decrease from 180 to 90 degrees/sec.
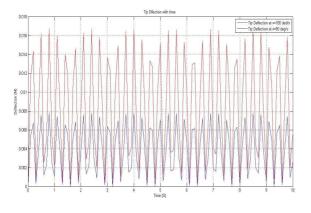

Fig. 11. Tip deflection at tip load=59.5 gram.

Fig. 11 shows the variation of tip deflection with time for two velocity (90 and 180)degree/sec. and for tip attached mass equals 59.5 gram. It shows that a time passes, the deflection fluctuates between a values. For v=90 degree/sec. blue curve, Maximum value was found to be (7.8 mm). For v=180 degree/sec. red curve, Maximum value was found to be (1.67cm).This figure also shows that the maximum tip deflection values decreases as the velocity of the servo motor decrease from 180 to 90 degrees/sec.

6.2. Experimental Results

The experimental results were obtained from the single link flexible manipulator and the tip deflection measured using accelerometer stick at the end of the link .The results were taken when the base servo motor operated at velocity equal (90,180) degrees/sec and for 120 degrees using servo motor control card GUI and for three different loads. The experimental results were shown below:
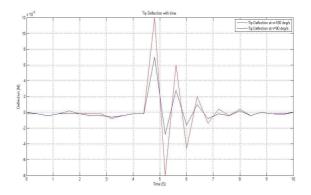

Fig. 12. Experimental tip deflection at tip load=0 gram.

Fig. 12 shows the variation of tip deflection with time for two velocity (90 and 180) degree/sec. and for tip attached mass equals zero gram. It shows that a time passes, the deflection fluctuates between a values. For v=90 degree/sec. blue curve, Maximum value was found to be (7 mm). For v=180 degree/sec. red curve, Maximum value was found to be (1.2cm).This figure also shows that the maximum tip deflection values decreases as the velocity of the servo motor decrease from 180 to 90 degrees/sec.
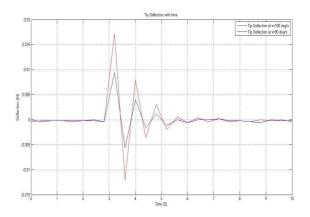

Fig. 13. Experimental tip deflection at tip load=27.4 gram.

Fig. 13 shows the variation of tip deflection with time for two velocity (90 and 180) degree/sec. and for tip attached mass equals 27.4 gram. It shows that a time passes, the deflection fluctuates between a values. For v=90 degree/sec. blue curve, Maximum value was found to be (9.4 mm). For v=180 degree/sec. red curve, Maximum value was found to be (1.72cm).This figure also shows that the maximum tip deflection values

decreases as the velocity of the servo motor decrease from 180 to 90 degrees/sec.

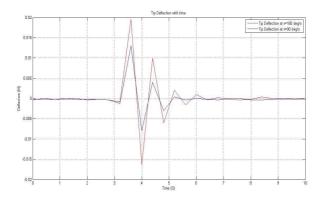**Fig. 14. Experimental tip deflection at tip load=59.5 gram.**

Fig. 14 shows the variation of tip deflection with time for two velocity (90 and 180) degree/sec. and for tip attached mass equals 59.5 gram. It shows that a time passes, the deflection fluctuates between a values. For v=90 degree/sec. blue curve, Maximum value was found to be (1.3 cm). For v=180 degree/sec. red curve, Maximum value was found to be (1.96cm).This figure also shows that the maximum tip deflection values decreases as the velocity of the servo motor decrease from 180 to 90 degrees/sec.

Table 2,
Theoretical &Experimental tip deflection result at different load.

Motor Velocity (deg/s)	Tip Load (gram)	Theoretical Max. Tip deflection (mm)	Experimental Max. Tip deflection(mm)	Percentage Difference
V=90	Zero	4.6	7	34 %
V=180		9.9	12	17.5%
V=90	27.4	6.1	9.4	35 %
V=180		13.1	17.2	23.8 %
V=90	59.5	7.8	13	40%
V=180		16.7	19.6	

7. Conclusions

The concluding remarks withdrawn from the obtained results as following:

- **Load:** maximum tip deflection of the flexible link increases as the tip attached mass increases from 0, 27.4 and 59.5 gram as shown in result obtained previously .
- **Velocity:** the deflection of the flexible link increases as the velocity of the base servo motor angle increases from [90-180] degrees/sec as shown in (Table:1).
- **Damping effect:** the damping effect is clear after approximately 5 second and obvious in the experimental results only because we neglect the damping effect at the theoretical part.

8. References

[1] Aarts R.G.K.M. and Jonker J.B.," Dynamic simulation of planar flexible link manipulators using adaptive modal integration", Multibody System Dynamics, Vol.7, pp. 31–50, 2002.

[2] Shaheed M.H. andTokhi M.O., "Dynamic modeling of a single-link flexible manipulator: parametric and non-parametric approaches" Robotica, Vol.20, pp. 93–109, 2002.

[3] Sciavicco, L., and Siciliano, B., "Modeling and Control of Robot Manipulators", Springer London, 2004.

[4] Book ,M.O. Tokhi and A.K.M. Azad,"Flexible Robot manipulator ,Modeling, Simulation and Control" , The Institution of Engineering and Technology, series 68 ,pp. 19-20,2008.

[5] Cannon R.H. and Schmitz E., "Initial experiments on end-point control of a flexible one-link robot", The International Journal of Robotics Research Vol.3, No.3, pp.62–75, 1984.

[6] Nagarajan S. and Turcic D.A., "Lagrangian formulation of the equations of motion for the elastic mechanisms with mutual dependencebetween rigid body and elastic motions", Part 1: Element level equations,

and Part II: System equations, ASME Journal of Dynamic Systems, Measurement, and Control, Vol.112, No. 2, pp.203–214, and pp.215–224, 1990.

[7] Choi S.B., Thompson B.S. and Gandhi M.V., "Modeling and control of a single-link flexible manipulator featuring a graphite–epoxycomposite arm", Proceedings of the IEEE International Conference on Robotics and Automation, Vol.2, pp.1450–1455, 1990.

[8] Choi, S.B., Gandhi, M.V. and Thompson,B. S., "An experimental investigation of an articulating robotic manipulator with a graphite epoxy arm". Journal of Robotic Systems, Vol.5, pp.73–79, 1988.

[9] Krishnamurthy K., Chandrashekhara K. and Roy S., "A study of single-link robots fabricated from orthotropic composite materials", Computers and Structures, Vol.136, No.1, pp.139–146, 1990.

[10] M. O. Tokhi and A. K. M. Azad,"Modelling of a single-link flexible manipulator system: theoretical and practical investigations", Robotica , V.14,No.1,pp.91-102,1996.

تحليل انحراف ذراع روبوت مرن احادي الوصلة

رفل محمد خليل*　　　　　　　**سومر متي داوود****

* قسم هندسة التصنيع المؤتمت/ كلية الهندسة الخوارزمي/ جامعة بغداد

** قسم هندسة الطب الحياتي/ كلية الهندسة الخوارزمي/ جامعة بغداد

البريد الالكتروني: Rafalalazzawi90@gmail.com

البريد الالكتروني: Somernacy@yahoo.com

الخلاصة

ان اطراف الروبوتات الصناعية ذات الهيكلية المرنه هي بديل اكثر فائدة مقارنة بأطراف الروبوتات الصناعية ذات الهيكلية الصلبة وان للعديد من التطبيقات الجديدة والمتطورة في مجال الروبوتات.في بعض التطبيقات استخدام الاطراف المرنه امر لا مفر منه و يقابل هذا زيادة في تعقيد التصميم والتحكم بهذه الاطراف لزيادة تحسين ادائها .في هذا البحث نقوم بتصميم وتنفيذ ذراع مرن واحد لروبوت صناعي وهذا الذراع مصنوع من مادة البايرسبكس بطول ٠.٥ متر ، عرض ٠.٠٢ متر وسمك ٠.٠٠٤ متر مع وجود كتلة مثبته في نهاية الذراع، هناك اربعة انظمة ثانوية هي: منظومة الحركة الثانويه و منظومة السيطرة الثانويه و منظومة الكمبيوتر وبرامجه الثانوية. ان مبدأ عمل ذراع الروبوت الصناعي المرن هو تدوير محرك السيرفو للقاعدة وهو يقوم بتدوير القاعدة ومعها الذراع المرن ونقيس الانحراف الذي يحصل في طرف الذراع ويقاس الانحراف في ثلاث حالات عند عدم وجود وزن في الطرف وعند وجود ٢٧.٤ و ٥٩.٥ غرام في طرف الذراع المرن وعند كل حالة من هذه الحالات نقوم بتحريك محرك السيرفو للقاعدة عند سرعة دورانية بمقدار ٩٠ درجه/ ثانيه بوساطة استخدام بطاقة تحكم بمحركات السيرفو التي تعمل على اساس متحكم (ATMEGA640) ونقيس الانحراف في طرف الذراع عند كل حالة من هذه الحالات بواسطة حساس للسرعه والدوران (MMA7631) وتتم السيطرة عليه بأستخدام لوحة اردينو (Mega2560) ثم نقوم بجمع البينات من حساس السرعه والدوران ورسمها ببرنامج الماتلاب والمقارنه بين النتائج النظرية التي حصلنا عليها من بناء برنامج بالماتلاب مبني على اساس معادلات لاكرانج للحركة والنتائج العملية التي حصلنا عليها .